ARTICLES

Effect of High-Frequency Modes and Hot Transitions on Free Energy Gap Dependence of Charge Recombination Rate

**Serguei V. Feskov, Vladimir N. Ionkin, and Anatoly I. Ivanov***

Department of Physics, Volgograd State University, University Avenue 100, Volgograd 400062, Russia

Received: May 28, 2006; In Final Form: August 27, 2006

The charge recombination (CR) dynamics of geminate ion pairs formed by excitation of the ground-state donor−acceptor complexes in polar solvent have been investigated within the framework of stochastic approach. It is shown that for low exergonic reactions these dynamics critically depend on the reorganization energy of intramolecular high-frequency mode. Even moderate reorganization energies (0.1−0.2 eV) significantly accelerate the excited-state population decay making it nearly exponential. In the solvent-controlled regime, the majority of the excited donor−acceptor complexes recombine at nonthermal (hot) stage when the nonequilibrium initial wave packet passes through a number of term crossings corresponding to the transitions with creation of several vibrational quanta. Analysis of this mechanism allows to conclude (i) the CR in viscous solvents proceeds much faster than the diffusive relaxation of solvent, (ii) under certain conditions, the CR rate becomes practically independent of the diffusive component of solvent relaxation which is determined by solvent viscosity, (iii) in contrast to predictions of Marcus theory, the CR rate decreases monotonically with the rise of reaction exergonicity even at small free energy gaps, in accordance with experimental results. Two semiquantitative approaches providing rather simple analytical expressions for the hot charge recombination dynamics are suggested. These approximations give a good reproduction of the excited-state decay in the wide area of model parameters.

I. Introduction

Primary photochemical reactions induced by excitation of the charge-transfer band in donor−acceptor complexes (DACs) may be described as in the scheme

$$DA \xrightarrow[k_{CR}]{h\nu} D^+A^- \xrightarrow{\varphi} D^+ + A^-$$
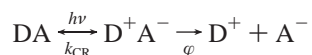
Here, $h\nu$ indicates the photoexcitation, k_{CR} is the charge recombination rate constant, and φ is the free ion quantum yield. Systematic experimental investigations of CR in excited DACs in polar solvents have shown an absence of the Marcus normal region in such reactions.[1−7] The rate constant of CR monotonically decreases with the rise of the reaction exothermicity throughout the accessible range of the reaction free energies -3 eV $< \Delta G_{CR} < -0.5$ eV.

An explanation of this phenomenon has been proposed in ref 8. It started from a reasonable assumption that excitation of the ground-state DAC by a short laser pulse produces a nonequilibrium excited state, which may be visualized as a wave packet lying above the point where the ground- and excited-state terms cross. Nuclear relaxation then can be imagined as the wave packet movement to the excited-state term minimum. If the free energy gap of recombination is not too large ($-\Delta G_{CR} < E_r$, where E_r is the reorganization energy), then the wave packet passes the term crossing region giving rise to electronic

transitions also known as nonthermal or hot transitions. In the case of strong electronic coupling, the majority of the excited-state DACs recombine at this hot stage, and the CR completes before the nuclear relaxation is over. This model reproduces well the experimentally observed free energy dependence of the CR rate.[8] There is one more piece of supporting evidence for this model: the relaxation of the ion state has been experimentally observed[2] as a shift of the excited-state absorption band maximum. Nevertheless, this simple model encounters two difficulties:[9] (i) a good fit requires too large values of electronic coupling at which diabatic description is no longer applicable, and (ii) the model predicts strong time dependence of the rate constant, in contradiction with most experimental data.

Large electronic coupling obtained from the fitting[8] pointed out that treatment of CR in DACs as a transition between the upper and lower adiabatic terms induced by the nonadiabatic interaction could be a more appropriate description. Such a theory was developed in ref 9. This theory could also reproduce well the experimentally observed free energy dependence of the CR rate constant. There is, however, a weak point in this theoretical explanation. Indeed, the time scale of CR in the low exergonic region is on the same order or even faster than that of the solvent relaxation, and therefore, the description should include an explicit consideration of the relaxation of the initial nonequilibrium nuclear distribution on the upper adiabatic free energy surface. Analysis of the nonequilibrium CR within the adiabatic model has shown[10] that this model predicts highly

---

* Corresponding author. E-mail: physic@vlink.ru.

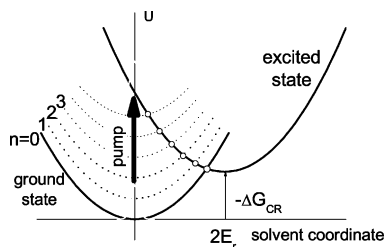**11920** *J. Phys. Chem. A, Vol. 110, No. 43, 2006*

Feskov et al.

Figure 1. The multichannel transfer to the ground state of DAC in the low exergonic region allowing the excitation of a number of sublevels of the high-frequency intramolecular vibrational mode (dashed lines). The ground-state distribution and the initial excited-state wave packet produced by a laser pump are also pictured.

nonexponential CR kinetics: the rate of the process is a fast-rising function of time. The upper state population decay within this model can be approximated by the function $P_e(t) = \exp[-(t/\tau)^s]$. For ultrafast CR in the low exergonic region, $-\Delta G_{CR} < E_r$, the parameter s is predicted to be rather large ($s > 1.5$),[10] so that the nonexponentiality of CR is expected to be considerably higher than that observed in experiments.[11,12]

Intramolecular high-frequency modes are well-known to play an important role in highly exergonic electron-transfer reactions in Marcus inverted region.[13-16] These modes may increase the rate constant of thermal reactions by a factor of several orders of magnitude. It is however believed that their role in the normal region is much less significant, and they are often ignored.

The situation is different for the nonthermal charge recombination reactions in DACs. This paper emphasizes the importance of the role played by the high-frequency modes in the low exergonic region, $-\Delta G_{CR} < E_r$, too. The mechanism is similar to that considered in ref 8 but accounts for multiple crossings between the excited diabatic state and vibrational sublevels of the ground state. The excited-state wave packet passes through these crossings, undergoing hot transitions at each of them. Owing to these transitions, the wave packet may disappear before its equilibration. As a result, the CR time scale is greatly reduced, and the rate of such nonthermal CR appears to be an increasing function of the reaction free energy, ΔG_{CR}, throughout the whole low exergonic region. A good fit to experimentally observed free energy gap dependence of the CR rate constant can be obtained with acceptable values of intramolecular reorganization energy and relatively weak electronic coupling when diabatic state representation is admissible. Rather unexpectedly, this model also predicts nearly exponential CR dynamics for the parameters obtained from fitting.

II. The Model and Numerical Method

We consider a DAC surrounded by a polar solvent and assume that only two electronic states of this complex can be populated in the charge separation/recombination processes—the ground state $|g\rangle$ and the excited (charge transfer) state $|e\rangle$. The system is initially in the ground state with the nuclear coordinates distributed according to the Boltzmann law. A nonzero dipole momentum of $|g\rangle \rightarrow |e\rangle$ transition leads to a vertical transfer of the initial population upon excitation of the charge-transfer band by a short laser pulse (Figure 1).

The newly formed nonequilibrium state of the system $|e\rangle$ is subjected to a series of relaxation processes in the nuclear subsystem; the reorganization of solvent and intramolecular vibrational degrees of freedom are of primary importance among them. It is commonly assumed that polar solvents, such as acetonitrile, have at least two relaxation components: the fast inertial component and the slower diffusive one.[17-19] This

implies that the solvent should be characterized by two relaxation time scales τ_1 and τ_2. Their values for acetonitrile are known to be $\tau_1 = 190$ fs[20] (inertial mode) and $\tau_2 = 500$ fs (diffusive mode). Defining the reaction coordinate of CR as a difference between the corresponding energy levels $\Delta E(t) = E_g - E_e$, one can describe the solvent relaxation through the autocorrelation function $K(t) = \langle \Delta E(t) \Delta E(0) \rangle$.[21,22] Using Markovian approximation for both the solvent modes, this function is written as[21,23]

$$K(t) = 2E_r k_B T X(t) \qquad (2.1)$$

where $E_r = E_{r1} + E_{r2}$ is the total reorganization energy, $X(t) = x_1 e^{-t/\tau_1} + x_2 e^{-t/\tau_2}$ is the function of solvent relaxation, $x_i = E_{ri}/E_r$, and E_{ri} is the reorganization energy of the ith mode.

Diabatic free energy surfaces for the electronic states in coordinates Q_1 and Q_2 are

$$U_g^{(n)} = \frac{Q_1^2}{4E_{r1}} + \frac{Q_2^2}{4E_{r2}} + n\hbar\Omega + \Delta G_{CR}$$

$$U_e = \frac{(Q_1 - 2E_{r1})^2}{4E_{r1}} + \frac{(Q_2 - 2E_{r2})^2}{4E_{r2}} \qquad (2.2)$$

where Ω is the frequency of the intramolecular quantum mode, and n is a number of a vibrational sublevel. Diabatic terms intersect along the lines $Q_1 + Q_2 = z_n^\dagger$, where $z_n^\dagger = E_r - \Delta G_{CR} - n\hbar\Omega$.

Thus, we are led to the problem of nonequilibrium electronic transitions. This is a long-standing problem which has been already addressed from different points of view.[8,24-37] Here, we need an approach which could allow us to calculate the CR dynamics in the case of strong electron transfer when the nonthermal electron-transfer probability is significant. The stochastic point–transition approach[21] generalized to the multilevel system is best suited to this aim.

We describe a temporal evolution of the system by a set of differential equations for the probability distribution functions for the excited state $\rho_e(Q_1, Q_2, t)$ and for nth sublevel ($n = 0, 1, 2, ...$) of the ground state $\rho_g^{(n)}(Q_1, Q_2, t)$

$$\frac{\partial \rho_e}{\partial t} = \hat{L}_e \rho_e - \sum_n k_n(Q_1, Q_2)(\rho_e - \rho_g^{(n)}) \qquad (2.3)$$

$$\frac{\partial \rho_g^{(n)}}{\partial t} = \hat{L}_g \rho_g^{(n)} - k_n(Q_1, Q_2)(\rho_g^{(n)} - \rho_e) + \frac{1}{\tau_v^{(n+1)}} \rho_v^{(n+1)} - \frac{1}{\tau_v^{(n)}} \rho_g^{(n)} \quad (n \neq 0) \ (2.4)$$

$$\frac{\partial \rho_g^{(0)}}{\partial t} = \hat{L}_g \rho_g^{(0)} - k_0(Q_1, Q_2)(\rho_g^{(0)} - \rho_e) + \frac{1}{\tau_v^{(1)}} \rho_g^{(0)} \quad (2.5)$$

where $\hat{L}_g$ and $\hat{L}_e$ are the Smoluchowski operators describing diffusion on U_g and U_e potentials

$$\hat{L}_g = \sum_{i=1}^{2} \frac{1}{\tau_i} \left(1 + Q_i \frac{\partial}{\partial Q_i} + \langle Q_i^2 \rangle \frac{\partial^2}{\partial Q_i^2} \right) \qquad (2.6)$$

$$\hat{L}_e = \sum_{i=1}^{2} \frac{1}{\tau_i} \left[1 + (Q_i - 2E_{ri}) \frac{\partial}{\partial Q_i} + \langle Q_i^2 \rangle \frac{\partial^2}{\partial Q_i^2} \right] \qquad (2.7)$$

CR Dynamics of Geminate Ion Pairs

J. Phys. Chem. A, Vol. 110, No. 43, 2006 **11921**

with $\langle Q_i^2 \rangle = 2E_{ri}k_BT$ being the dispersion of the equilibrium distribution along the ith coordinate, and k_B and T being the Boltzmann constant and bath temperature. $z = Q_1 + Q_2$ is the collective energetic coordinate of the reaction. Coupling parameters $k_n(Q_1, Q_2)$ are the Zusman rates of electron transfer between the excited state $|e\rangle$ and the nth vibrational sublevel of the ground state $|g\rangle$

$$k_n = \frac{2\pi V_n^2}{\hbar} \delta(U_e - U_g^{(n)}) = \frac{2\pi V_n^2}{\hbar} \delta(z - z_n^\dagger)$$

$$V_n^2 = V_{el}^2 \frac{S^n e^{-S}}{n!} \tag{2.8}$$

where $S = E_{rv}/\hbar\Omega$ and E_{rv} are the Huang−Rhys factor and the reorganization energy of the high-frequency vibrational mode, respectively. We adopt here a single-quantum mechanism of high-frequency mode relaxation and the transitions $n \rightarrow n - 1$ to proceed with the rate constant $1/\tau_v^{(n)}$, where

$$\tau_v^{(n)} = \tau_v^{(1)}/n \quad (n = 1, 2, ...) \tag{2.9}$$

To the best of our knowledge, there are no reliable experimental data on dependence of $\tau_v^{(n)}$ on the number of vibrational quanta, n. However, the decay of highly excited vibrational states is known to proceed mainly through intramolecular vibrational redistribution (IVR). If we suppose the cubic anharmonism to be the key reason of IVR in a large molecule, then simple estimations lead to eq 2.9.

To specify the initial conditions, we assume that the pump pulse is short enough, with the spectral width larger than $(2E_r k_B T)^{1/2}$. This implies vertical transfer of the equilibrium Boltzmann distribution to the excited term

$$\rho_e(Q_1, Q_2, t = 0) =$$

$$\frac{1}{2\pi \sqrt{\langle Q_1^2 \rangle \langle Q_2^2 \rangle}} \exp\left[-\frac{Q_1^2}{2\langle Q_1^2 \rangle} - \frac{Q_2^2}{2\langle Q_2^2 \rangle} \right] \tag{2.10}$$

The system of eqs 2.3−2.5 with the initial condition eq 2.10 was solved numerically using the Brownian simulation method.[11,38] We run 10^5 trajectories to obtain the necessary convergence of the results. The QM2L software is available on the Web (http://physics.volsu.ru/feskov/software).

Notice that a model very close to that considered here was studied in ref 16. There is, however, an important difference between them. Equations 2.3−2.5 account for the local reversibility of the reaction which plays a significant role in the strong coupling limit.[39,40] Since the typical values of the electronic coupling V_{el} in DACs are rather large, we address here the strong CR reactions in the low exergonic region where the reaction reversibility can crucially alter the CR dynamics.

The reversibility can be adequately accounted for within this model only if the intramolecular vibrational relaxation or the vibrational redistribution is also taken into account. The IVR is well-known to proceed on the time scale of $\tau_v < 100$ fs.[41] Equations 2.3−2.10 account for the IVR through the parameter $\tau_v^{(n)}$. Its variation alters the CR regime from the totally irreversible ($\tau_v^{(n)} \rightarrow 0$) to the reversible one ($\tau_v^{(n)} \rightarrow \infty$). Of course, the transition to the level $n = 0$ is reversible irrespective of the magnitude of τ_v (see eq 2.5).

III. Simulation Results and Discussion

Charge Recombination Dynamics. Electronic Coupling Effect. The results of simulations of the CR dynamics with
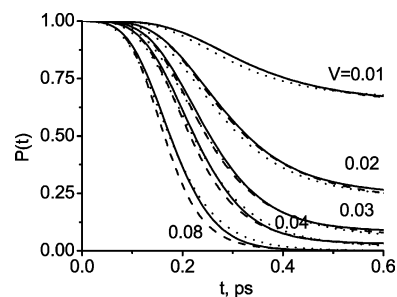

Figure 2. The time dependence of the excited-state population for a number of electronic coupling values calculated using the exact numerical simulations (solid curves), the time-dependent rate constant approach eq 24 (dashed curves), and the nonthermal electron-transfer probability approach eq 29 (dotted curves). The electron coupling values in electronvolts are indicated near the curves. Other parameters are as follows: $\Omega = 0.1$ eV, $E_r = 1$ eV, $\Delta G_{CR} = -0.5$ eV, $S = 3$, $x_1 = x_2 = 0.5$, $\tau_1 = 190$ fs, $\tau_2 = 500$ fs, $\tau_v^{(1)} = 70$ fs, $T = 300$ K.
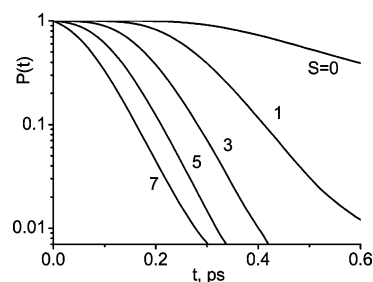

Figure 3. The time dependence of the excited-state population for a number of reorganization energy values of intramolecular quantum mode. The values of the Huang−Rhys parameter are indicated near the curves. Other parameters are as follows: $V_{el} = 0.08$ eV, $\Omega = 0.1$ eV, $E_r = 1$ eV, $\Delta G_{CR} = -0.5$ eV, $x_1 = x_2 = 0.5$, $\tau_1 = 190$ fs, $\tau_2 = 500$ fs, $\tau_v^{(1)} = 70$ fs, $T = 300$ K.

different values of V_{el} are presented in Figure 2. Here, we used typical values of the model parameters characteristic to DACs in a strongly polar solvent like acetonitrile. These parameters are indicated in the figure caption.

The excited-state population dynamics are well-separated into two stages. The hot stage is terminated when the wave packet passes the lowest term crossing point (see Figure 1). At the second (thermal) stage, the CR proceeds as an activated reaction, with a much smaller rate. Figure 2 also shows that more than 97% of the excited DACs recombine at the hot stage if the electronic coupling exceeds 0.04 eV. This implies that the thermal stage can be practically unobservable in such reactions.

The hot stage also has two phases. Obviously, the system needs some time to reach the region where the hot transitions take place with the significant rates. This phase is seen as a plateau at the short time scale. At the later phase, the model predicts rather fast decay of the excited-state population with the rate constant of $k \simeq 19$ ps^{-1} for $V_{el} = 0.08$ eV.

The mechanism of the influence of electronic coupling strength V_{el} on the CR is straightforward. Increase of V_{el} makes the sinks at the $z_n^\dagger$ points more effective and the relative amount of systems undergoing transitions to the states with larger n increases. This mechanism is also responsible for the shortening of the plateau and the rise of the effective rate constant.

Role of Intramolecular Vibrations. The influence of the reorganization energy of the high-frequency vibrational mode E_{rv} on the CR dynamics is pictured in Figure 3. Increase of E_{rv} profoundly accelerates the CR, compressing the time interval at which the excited-state population remains almost constant. Figure 3 shows that even mode with reorganization energy as
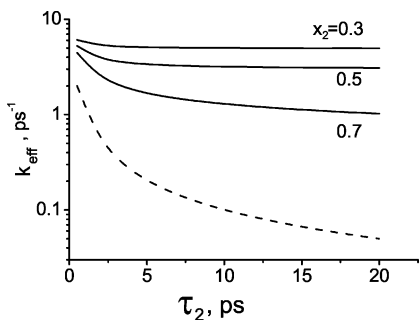
11922 *J. Phys. Chem. A, Vol. 110, No. 43, 2006*

Feskov et al.

Figure 4. Influence of the diffusive relaxation time of the solvent on the excited-state population decay dynamics. The values of the diffusive mode weight, x_2, are indicated near the curves. For comparison, the function $1/\tau_2$ is pictured as the dashed line. Other parameters are as follows: $V_{el} = 0.08$ eV, $\Omega = 0.1$ eV, $S = 3$, $E_r = 1$ eV, $x_1 + x_2 = 1$, $\Delta G_{CR} = -0.5$ eV, $\tau_1 = 190$ fs, $\tau_v^{(1)} = 70$ fs, $T = 300$ K.

small as 0.1 eV considerably changes the CR dynamics. With further rise of E_{rv}, the CR kinetics come closer to the exponential regime. It should be noticed that exponential decay is an inherent feature of equilibrium kinetics, but here we see very similar kinetics in a highly nonequilibrium process.

When $S = 0$, there is a single operative sink, corresponding to intersection of the U_e and $U_g^{(0)}$ terms. Passage of the wave packet through this intersection induces a pulsed rise of the CR rate, because the rate is proportional to the excited-state population at the term crossing point. As a result, a pronounced nonexponentiality of excited-state decay is expected. On the other hand, increase of the Huang–Rhys factor S enhances the power of the above-lying sinks with $n > 0$. This opens up new reaction channels associated with excitation of intramolecular vibrations in the ground-state DACs. This mechanism is responsible for the acceleration of hot CR in the strong electron-transfer regime.

Solvent Effects. The biexponential character of the solvent relaxation (eq 2.1) gives rise to some dynamical effects in the hot CR which are discussed in this chapter. It is commonly accepted that the inertial relaxation component is present at most known polar solvents and is practically independent of their nature.[42,43] On the other hand, the time scale of the slower diffusive component varies over a wide range. The roles of these modes in the CR reactions depend on the relative weights x_i, but, by not the least extent, they depend on the reaction free energy ΔG_{CR}. Indeed, the parameters x_i determine the "trajectory" of the wave packet descent downward the excited-state term minimum. The wave packet reaches the $Q_1 + Q_2 = z_n^\dagger$ crossing line at the moment t_n which can be found from the equation

$$2E_r X(t_n) = E_r + \Delta G_{CR} + n\hbar\Omega. \qquad (3.1)$$

If $\tau_2 \gg \tau_1$, then the fast and the slow relaxation phases are well-separated. Let n_0 be the number of the lowest ground state sublevel that is reached after relaxation of the fast mode. It can be found from eq 3.1 if we set $X(t_{n_0}) = x_2$. One obtains $n_0 = 9$ for $x_1 = 0.3$, $n_0 = 5$ for $x_1 = 0.5$, and $n_0 = 1$ for $x_1 = 0.7$. The latter value of n_0 means that at $x_1 = 0.7$ the packet passes almost all the crossings during the fast relaxation phase. In this case, the diffusive reorganization of the solvent remains nearly frozen in the course of the hot transitions and does not affect their dynamics significantly.

A similar effect can be expected if the packet reaches the most effective sinks $z_n^\dagger$, located around $n = [S]$, during the fast

relaxation phase. This is true if the following condition is met

$$2E_r x_2 < E_r + \Delta G_{CR} + S\hbar\Omega \qquad (3.2)$$

In this case, the rate of charge recombination remains rather high even at $t > \tau_1$. This results in fast decay of the excited-state population, almost independently of the particular value of τ_2.

The above reasoning is illustrated by simulations presented in Figure 4. Here, we calculated the dependence of the effective rate constant k_{eff} on the diffusive relaxation time scale τ_2, assuming τ_1 to be fixed. The three solid curves in this figure correspond to $x_1 = 0.3$, 0.5, and 0.7. The quantity k_{eff} is determined by the equation

$$k_{eff}^{-1} = \int_0^\infty P_e(t)\, dt \qquad (3.3)$$

where

$$P_e(t) = \int\int dQ_1\, dQ_2 \rho_e(Q_1, Q_2, t) \qquad (3.4)$$

is the time-dependent population of the excited state. The two upper curves in the figure clearly demonstrate the relatively small decrease of the rate in the region $\tau_2 \approx \tau_1$, and it is nearly independent of τ_2 when $\tau_2 \gg \tau_1$. For the third curve with $x_1 = 0.3$, there is no such saturation in the region of large τ_2, but the dependence still remains much weaker than the $1/\tau_2$ dependence, following from the thermal theory in the absence of inertial mode.[21]

The following conclusions can be summarized from these results: (i) The effective CR rate is considerably larger than the maximal thermal rate predicted by Zusman theory,[21,44] $k_{max} \simeq 1/\tau_2 = 1/\tau_L$, where τ_L is the longitudinal dielectric relaxation time. (ii) The pronounced τ_2 dependence of k_{eff} can be observed only in solvents with a relatively large weight of the slow mode ($x_2 > 0.5$).

It would also be informative to see the relative numbers ϕ_n of the excited particles that undergo hot recombination through the nth reaction channel. These results are pictured in Figure 5 as the distribution histograms. One can see that the increase of τ_2 results in narrowing of the distribution, the states with smaller n becoming less populated but the population of the states with larger n being slightly variable. These changes of the distribution come into particular prominence when the magnitude of x_1 is decreased.

One can also see only a minor dependence of the ϕ_n distribution on τ_2 for $x_1 = 0.7$, because a large share of hot transitions occurs at the fast phase. On the other hand, for $x_1 = 0.3$ a considerable redistribution of hot transitions toward the higher-lying sinks is observed with the rise of τ_2.

Free Energy Gap Dependence of the CR Rate in the Low Exergonic Region. Experimental investigations of many excited DACs have shown a nearly linear free energy dependence of the CR rate in the logarithmic scale.[1-7] The slope of the free energy dependence for DACs investigated by Mataga and co-workers was found to be around -1.35 decade/eV.[1] Smaller values of the slope (up to zero) were also observed.[6] We investigated such dependence numerically within the above model. The results are presented in Figure 6.

The main conclusions of these investigations are as follows: (i) Variation of x_1 and V_{el} leads to the vertical shift of the curve with minor modification of its shape. (ii) Decrease of the parameters Ω, E_{rv}, and E_r decreases the slope but at the same time results in considerable deviations from the linear dependence. The most appropriate fit to the Mataga's data is obtained
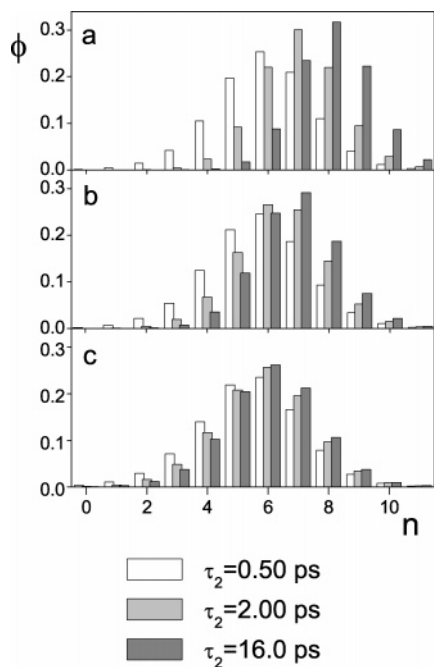
CR Dynamics of Geminate Ion Pairs

J. Phys. Chem. A, Vol. 110, No. 43, 2006 **11923**

Figure 5. Distributions of the ground-state DAC yields associated with the creation of n high-frequency vibrational quanta, ϕ_n, for a number of x_1 values. $x_1 = 0.3$ (a), $x_1 = 0.5$ (b), and $x_1 = 0.7$ (c). Other parameters are the same as in Figure 4.
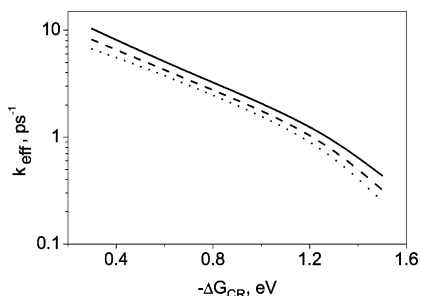

Figure 6. The free energy dependence of the CR rate constant for a number of electron coupling values. $V_{el} = 0.07$ eV (solid line), $V_{el} = 0.05$ eV (dashed line), and $V_{el} = 0.04$ eV (dotted line). Other parameters are as follows: $\Omega = 0.1$ eV, $S = 3$, $E_r = 0.5$ eV, $x_1 = x_2 = 0.5$, $\tau_1 = 190$ fs, $\tau_2 = 500$ fs, $\tau_v^{(1)} = 70$ fs, $T = 300$ K.

for the parameters presented in the Figure 6 caption. It is worth noting that the best fit parameters are close to the most typical values of E_r and E_{rv} for DACs in polar solvents.[5]

IV. Semiquantitative Approaches

The underlying physics of the above numerical results are rather transparent. Hence, it would be useful to construct analytical approaches highlighting the nature of the phenomena. Here, we suggest two approaches addressing the problem from the different points of view. The first uses the concept of the time-dependent rate of the reaction, and the second exploits the nonthermal transition probabilities.

The Time-Dependent Rate Constant Approach. Existing theories of activated electron transfer in condensed media describe the process in terms of the rate constant k which is commonly represented as a product of the pre-exponent, A, and the Arrhenius factor

$$k = A \exp(-E_a/k_B T) \tag{4.1}$$

where $E_a = (E_r + \Delta G_{CR})^2/4E_r$ is the activation energy of the reaction. This expression can be recast in the form

$$k = k_{intr} \rho(z^{\dagger}) \tag{4.2}$$

where $\rho(z^{\dagger})$ is the equilibrium population of particles at the term crossing point $z^{\dagger} = E_r + \Delta G_{CR}$, and k_{intr} is the "intrinsic" rate constant. Indeed, the electron-transfer dynamics are determined by both the number of particles "ready" for the reaction ($\rho(z^{\dagger})$) and the efficiency of their transitions (k_{intr}).

The first multiplier in eq 4.2, k_{intr}, in fact accounts for a variety of phenomena, including quantum tunneling of electrons between the donor and acceptor molecules, multiple recrossings of the $z^{\dagger}$, local reversibility of the reaction, and so forth. The quantity k_{intr} is proportional to V_{el}^2 within the golden rule limit and becomes independent of V_{el} in the solvent-controlled regime.[21,44] These two limits are combined within the Zusman theory that provides the following equation for the thermal rate constant[21]

$$k_{zus} = \frac{V_{el}^2}{\hbar(1+g)} \sqrt{\frac{\pi}{E_r k_B T}} \exp\left[-\frac{E_a}{k_B T}\right] \tag{4.3}$$

where

$$g = \frac{2\pi V_{el}^2 \tau_L}{\hbar}\left(\frac{1}{E_r + \Delta G_{CR}} + \frac{1}{E_r - \Delta G_{CR}}\right) \tag{4.4}$$

Irreversible variant of this expression differs from the above equation only by g, which in this case takes the form

$$g_{irr} = \frac{2\pi V_{el}^2 \tau_L}{\hbar(E_r + \Delta G_{CR})}$$

This approach can be easily generalized to the hot electronic transitions as well. This can be done by replacement of the equilibrium Boltzmann distribution in eq 4.2 by the time-dependent one, $\rho(z^{\dagger}, t)$, reflecting the wave packet relaxation to the bottom of the excited-state surface.

To do this, we turn to a one-dimensional description with the single collective coordinate $z = Q_1 + Q_2$. Relaxation of the initial wave packet in the absence of electronic transitions ($k_n = 0$) is then given by the equation

$$\rho_e^0(z, t) = \frac{1}{\sqrt{2\pi\langle z^2\rangle}} \exp\left\{-\frac{[z - M_z(t)]^2}{2\langle z^2\rangle}\right\} \tag{4.5}$$

where

$$M_z(t) = 2E_r[1 - X(t)] \tag{4.6}$$

is the time-dependent position of the wave packet maximum, and $\langle z^2\rangle = 2E_r k_B T$ is its thermal width.

Accounting for a number of term intersections at the $z_n^{\dagger}$ points, we rewrite the total CR rate as a sum of partial rates $k_z^{(n)}(t)$ corresponding to the electronic transitions to nth vibrational sublevel

$$k_z(t) = \sum_n k_z^{(n)}(t) = \sum_n \frac{2\pi V_n^2}{\hbar(1 + \tilde{g}_n)} \rho_e^0(z_n^{\dagger}, t) \tag{4.7}$$

Here

$$V_n^2 = V_{el}^2 \frac{S^n}{n!} e^{-S} \quad \tilde{g}_n = \tilde{g}\frac{S^n}{n!} e^{-S} \tag{4.8}$$

and $\tilde{g}$ differs from g (eq 4.4) by substitution of the effective solvent relaxation time $\tilde{\tau}$ for τ_L[45,46]

$$\frac{1}{\tilde{\tau}} = \frac{x_1}{\tau_1} + \frac{x_2}{\tau_2} \tag{4.9}$$

The excited-state population is then easily calculated as

$$P_z(t) = \exp[-\int_0^t k_z(t')\,dt'] \tag{.4.10}$$

Good quantitative agreement between this approach and the exact numerical simulations has been obtained in a wide area of model parameters. An example of this estimation is shown in Figure 2 (dashed curves) where we used the irreversible variant of eq 4.3 for the comparison. This indicates that the concept of the "intrinsic" rate constant worked out for thermal electron transfer theory may be successfully applied to the hot transfer as well. This analytical approach excellently reproduces the time-dependent CR rate in the case of weak and moderate electron transfer and slightly overestimates the rate in the solvent-controlled regime.

Nonthermal Electron Transfer Probability Approach. If we think of the CR process as a series of hot electronic transitions at the term crossings, $z_n^{\dagger}$, we can suggest another simple and effective method for the CR dynamics calculations. It uses known analytical expressions for the nonthermal electronic transition probabilities.[39,47]

Since the motion along both solvent modes is Markovian, the descent of the excited-state wave packet to the term minimum is

$$\bar{Q}_1(t) = 2E_{r1}(1 - e^{-t/\tau_1})$$

$$\bar{Q}_2(t) = 2E_{r2}(1 - e^{-t/\tau_2}) \tag{4.11}$$

The packet encounters the nth term crossing line at the moment t_n, which is the solution of the transcendent eq 3.1. Passage of the wave packet through this line results in "loss" of population due to the hot CR. The probability of this transition is determined by the equation[39,47]

$$W_n = \frac{2\pi V_n^2}{A_{1n}^{(1)} + A_{2n}^{(1)}}\left\{1 + 2\pi V_n^2\left[\frac{1}{A_{1n}^{(1)} + A_{2n}^{(1)}} + \frac{1}{|A_{1n}^{(2)} + A_{2n}^{(2)}|}\right]\right\}^{-1} \tag{4.12}$$

where

$$A_{in}^{(1)} = \frac{\bar{Q}_i(t_n)}{\tau_i} \quad A_{in}^{(2)} = \frac{\bar{Q}_i(t_n) - 2E_{ri}}{\tau_i} \quad i = 1, 2 \tag{4.13}$$

are the slopes of the terms at the point $(\bar{Q}_1(t_n), \bar{Q}_2(t_n))$. For irreversible reactions, this equation is modified by setting the last term in the square brackets in eq 4.12 equal to zero.

The excited-state population distribution, $\rho_e(Q_1, Q_2, t)$, can now be approximated by the equation

$$\rho_e(Q_1, Q_2, t) \simeq \rho_e^{(0)}(Q_1, Q_2, t)\prod_{n=0}^{\infty}[1 - W_n\theta(Q_1 + Q_2 - z_n^{\dagger})] \tag{4.14}$$

where $\rho_e^{(0)}(Q_1, Q_2, t)$ is the solution of eq 2.3 in the absence of electronic transitions, $\theta(x)$ is the Heaviside step function.

Inserting eq 4.14 into eq 3.4, we finally obtain the following analytic expression for the excited-state population dynamics

$$P_w(t) = \frac{p_0}{2}\,\mathrm{erfc}(\zeta_0(t)) +$$

$$\sum_{m=1}^{\infty}\frac{p_m}{2}[\mathrm{erfc}(\zeta_m(t)) - \mathrm{erfc}(\zeta_{m-1}(t))] \tag{4.15}$$

where $p_m = \Pi_{n=m}^{\infty}(1 - W_n)$ is the total probability of survival after passing the mth crossing line

$$\zeta_m(t) = \frac{z_m^{\dagger} - M_z(t)}{\sqrt{2\langle z^2\rangle}}$$

and

$$\mathrm{erfc}(x) = \frac{2}{\sqrt{\pi}}\int_x^{\infty}e^{-t^2}\,dt$$

is the complementary error function.

If the activation barrier of the thermal CR is large, $(E_r + \Delta G_{CR})^2/(4E_r k_B T) \gg 1$, then the hot stage and the thermal stage are well-separated. In this case, the long-time asymptote of eq 4.15 gives the hot CR quantum yield, $P_w(t \to \infty) = p_0$, which is the total survival probability to reach the bottom of the excited-state surface.

The results of calculations of $P_w(t)$ are pictured in Figure 2 (dotted lines). It is seen that this approach describes well both the hot CR dynamics and quantum yield. It should be emphasized that eq 4.15 accounts for the hot transitions only, so the approach is expected to provide a good description in the low exergonic region and to fail when the CR approaches the barrierless region ($-\Delta G_{CR} \approx E_r$).

V. Conclusion Remarks

In this paper, we have investigated a model of the CR of the excited DACs in the nonadiabatic regime. The hot electronic transitions assisted by reorganization of the intramolecular high-frequency quantum mode, and the solvent relaxation involving both the fast inertial and slow diffusive components has been shown to radically alter the CR dynamics. The main conclusions can be summarized as follows.

1. Multichannel hot transitions enhance the CR rate in the low exergonic region overturning the ascending branch of the Marcus inverted parabola. As a result, the CR rate constant monotonically decreases with the free energy gap in the strong coupling regime.

2. The intramolecular reorganization combined with the inertial solvent relaxation approaches the excited-state decay to the exponential regime.

3. In solvents with relatively large weight of the inertial mode ($x_1 > 0.5$), there is a minor dependence of the CR rate constant on the diffusive solvation time scale. Thus, the model predicts only a weak dependence of the CR rate on the solvent viscosity.

An important point to emphasize is that the successful fits to the free energy gap dependence of the CR rate in excited DACs were obtained within the frameworks of nonadiabatic theories,[7,8,16] but they were achieved with very strong electronic couplings lying far beyond the limits of the nonadiabatic theory applicability. Our best fit parameters fall within the applicability area. Indeed, the stochastic approach is also based on the diabatic representation, and hence, its applicability is limited by the relatively weak electronic couplings. However, even with the

CR Dynamics of Geminate Ion Pairs

J. Phys. Chem. A, Vol. 110, No. 43, 2006 **11925**

largest value, $V_{el} = 0.08$ eV, for all controlling transitions (see Figure 5), the applicability condition, which can be roughly estimated as $V_n < k_BT$,[36] is not violated.

So, there are two alternative, adiabatic (transitions between the upper and lower adiabatic states)[8,10] and nonadiabatic (transitions between the weakly coupled diabatic states), theories providing an explanation for the absence of normal region in CR dynamics of excited DACs. Apparently, at the moment, it is not possible to uniquely establish which alternative is actually realized in DACs. We may only summarize evidence in favor of either theory. Estimations of the electronic coupling in DACs give large values[4,5] that support the adiabatic theory. On the other hand, strong electronic coupling implies that there is no complete charge separation in the excited state, and nuclear relaxation accompanying the excitation of a DAC has to result in considerable decrease of the ion charges, in contrast to experimental data which verify that the excited DACs evolve into a contact ion pair with full charge separation.[48,49] The positive spectral effect (increase of the CR rate with the rise of the carrier frequency of the pumping pulse) observed in excited DACs[11,12] also supports the nonadiabatic theory, because it is not expected within the adiabatic theory.[10]

References and Notes

(1) Asahi, T.; Mataga, N. *J. Phys. Chem.* **1989**, *93*, 6575.

(2) Asahi, T.; Mataga, N. *J. Phys. Chem.* **1991**, *95*, 1956.

(3) Segawa, H.; Takehara, C.; Honda, K.; Shimidzu, T.; Asahi, T.; Mataga, N. *J. Phys. Chem.* **1992**, *99*, 503.

(4) Benniston, C. A.; Harriman, A.; Philp, D.; Stoddart, J. F. *J. Am. Chem. Soc.* **1993**, *115*, 5298.

(5) Gould, I. R.; Noukakis, D.; Gomez-Jahn, L.; Goodman, J. L.; Farid, S. *J. Am. Chem. Soc.* **1993**, *115*, 4405.

(6) Hubig, S. M.; Bockman, T. M.; Kochi, J. K. *J. Am. Chem. Soc.* **1996**, *118*, 3842.

(7) Nicolet, O.; Vauthey, E. *J. Phys. Chem. A* **2002**, *106*, 5553.

(8) Tachiya, M.; Murata, S. *J. Am. Chem. Soc.* **1994**, *116*, 2434.

(9) Frantsuzov, P. A.; Tachiya, M. *J. Chem. Phys.* **2000**, *112*, 4216.

(10) Mikhailova, V. A.; Ivanov, A. I.; Vauthey, E. *J. Chem. Phys.* **2004**, *121*, 6463.

(11) Fedunov, R. G.; Feskov, S. V.; Ivanov, A. I.; Nicolet, O.; Pagès, S.; Vauthey, E. *J. Chem. Phys.* **2004**, *121*, 3643.

(12) Nicolet, O.; Banerji, N.; Pagès, S.; Vauthey, E. *J. Phys. Chem. A* **2005**, *109*, 8236.

(13) Walker, G. C.; Akesson, E.; Johnson, A. E.; Levinger, N. E.; Barbara, P. F. *J. Phys. Chem.* **1992**, *96*, 3728.

(14) Barbara, P. F.; Walker, G. C.; Smith, T. P. *Science* **1992**, *256*, 975.

(15) Denny, R. A.; Bagchi, B.; Barbara, P. F. *J. Chem. Phys.* **2001**, *115*, 6058.

(16) Bagchi, B.; Gayathry, N. *Adv. Chem. Phys.* **1999**, *107*, 1.

(17) Rosenthal, S. J.; Xie, X.; Du, M.; Fleming, G. R. *J. Chem. Phys.* **1991**, *95*, 4715.

(18) Maroncelli, M.; Kumar, V. P.; Papazyan, A. *J. Phys. Chem.* **1993**, *97*, 13.

(19) Jimenez, R.; Fleming, G. R.; Kumar, P. V.; Maroncelli, M. *Nature (London)* **1994**, *369*, 471.

(20) Passino, S. A.; Nagasawa, Y.; Fleming, G. R. *J. Phys. Chem.* **1997**, *101*, 725.

(21) Zusman, L. D. *Chem. Phys.* **1980**, *49*, 295.

(22) Burshtein, A. I.; Yakobson, B. I. *Chem. Phys.* **1980**, *49*, 385.

(23) Garg, S.; Smith, C. *J. Phys. Chem.* **1965**, *69*, 1294.

(24) Bakhshiev, N. G. *Opt. Spectrosc.* **1964**, *16*, 446.

(25) Hizhnyakov, V.; Tekhver, I. Yu. *Phys. Status Solidi* **1967**, *21*, 75.

(26) Mazurenko, Yu. T.; Bakhshiev, N. G. *Opt. Spectrosc.* **1970**, *28*, 490.

(27) Zusman, L. D.; Helman, A. B. *Opt. Spectrosc.* **1982**, *53*, 248.

(28) Bagchi, B.; Oxtoby, D. W.; Fleming, G. R. *Chem. Phys.* **1984**, *86*, 25.

(29) Van der Zwan, G.; Hynes, J. T. *J. Phys. Chem.* **1985**, *89*, 4181.

(30) Loring, R. F.; Yan, Y. J.; Mukamel, S. *J. Chem. Phys.* **1987**, *87*, 5840.

(31) Najbar, J.; Dorfman, R. C.; Fayer, M. D. *J. Chem. Phys.* **1991**, *94*, 1081.

(32) Coalson, R. D.; Evans, D. G.; Nitzan, A. *J. Chem. Phys.* **1994**, *101*, 436.

(33) Cho, M.; Silbey, R. J. *J. Chem. Phys.* **1995**, *103*, 595.

(34) Domcke, W.; Stock, G. *Adv. Chem. Phys.* **1997**, *100*, 1.

(35) Jean, J. M. *J. Phys. Chem. A* **1998**, *102*, 7549.

(36) Barzykin, A. V.; Frantsuzov, P. A.; Seki, K.; Tachiya, M. *Adv. Chem. Phys.* **2002**, *123*, 511.

(37) Ivanov, A. I.; Belikeev, F. N.; Fedunov, R. G.; Vauthey, E. *Chem. Phys. Lett.* **2003**, *372*, 73.

(38) Gladkikh, V.; Burshtein, A. I.; Feskov, S. V.; Ivanov, A. I.; Vauthey, E. *J. Chem. Phys.* **2005**, *123*, 244510.

(39) Feskov, S. V.; Ivanov, A. I.; Burshtein, A. I. *J. Chem. Phys.* **2005**, *122*, 124509.

(40) Frauenfelder, H.; Wolynes, P. G. *Science* **1985**, *229*, 337.

(41) Kovalenko, S. A.; Schanz, R.; Hennig, H.; Ernsting, N. P. *J. Chem. Phys.* **2001**, *115*, 3256.

(42) Chapman, C. F.; Fee, R. S.; Maroncelli, M. *J. Phys. Chem.* **1990**, *94*, 4929.

(43) Fee, R. S.; Maroncelli, M. *Chem. Phys.* **1994**, *183*, 235.

(44) Rips, I.; Jortner, J. *J. Chem. Phys.* **1987**, *87*, 6513.

(45) Hynes, J. T. *J. Phys. Chem.* **1986**, *90*, 3701.

(46) Bicout, D. J.; Szabo, A. *J. Chem. Phys.* **1997**, *109*, 2325.

(47) Ivanov, A. I.; Potovoi, V. V. *Chem. Phys.* **1999**, *247*, 245.

(48) Asahi, T.; Ohkohchi, M.; Mataga, N. *J. Phys. Chem.* **1993**, *97*, 13132.

(49) Mataga, N.; Miyasaka, H. *Adv. Chem. Phys.* **1999**, *107*, 431.